446. On the Kinematics and Dynamics of 3-DOF Parallel Robots with Triangle Platform

Tiberiu Itul[1,a], Doina Pisla[1,b]
[1]Technical University of Cluj-Napoca, Constantin Daicoviciu 15, RO-400020 Cluj-Napoca, Romania
e-mail: [a]*itultp@yahoo.com;* [b]*doinapisla@yahoo.com*

(Received 14 January 2009; accepted 10 March 2009)

Abstract. In the first part of the paper a structural study of two types of 3-DOF parallel mechanisms with triangle platform is reported. A comparison between their geometric models is performed. Kinematics and dynamics using Newton-Euler formalism for a concrete case of 3-RRS parallel structure used for orientation applications (TV satellite antenna or sun tracker) are presented. In order to get the drive torques, which are necessary to overcome the frictions from the joints, the principle of virtual power is applied. The algorithms and simulation results for the workspace and singularities generation are provided. Diagrams for the dynamics representation are computed by means of numerical and graphical simulations.

Keywords: parallel robots, kinematics, dynamics, workspace, singularities, friction.

Introduction

Parallel kinematic structures have a series of advantages that makes them adequate for construction of mini-robots and micro-robots: actuator positioning on the seating, miniaturization, stiffness, positioning precision and repeatability, actuators separation from the workspace. For these reasons more and more parallel mechanisms with specified number and type of degrees of freedom have been proposed and studied [2-20].

In [1] the 3-DOF spatial parallel symmetrical and guided mechanisms are defined. Structural archetype schemes of the "a" and "b" type guided in three points parallel mechanisms are presented in the figure 1.

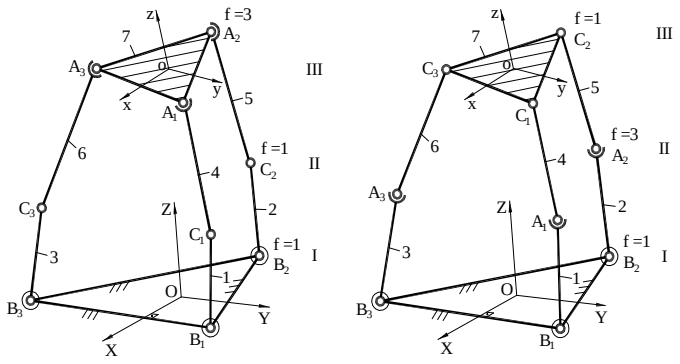

Fig. 1. The "a" and "b" type parallel mechanisms

The joints surrounded by circles, which are located in the proximity of the fixed base, suggest that these joints are actuated, each of them having 1 DOF. Each kinematic chain, which connects the fixed base with the mobile platform, contains also a passive joint with 1 DOF and a passive spherical joint with 3 DOF. Spherical joints centers are conventionally called guiding points. In the case of the "a" type mechanisms, the guiding points A_i (i=1,2,3) are moving, each of them on single DOF curve with respect to the base. In the case of the "b" type mechanisms, the guiding points A_i (i=1, 2, 3) are moving, each of them on a fixed curve jointed with the base respectively on a curve jointed with the mobile plate. The actuating joints with 1 DOF could be "R"-revolute or "P"-prismatic.

Kinematic Analysis

To the $B_1B_2B_3$ fixed base the $OXYZ$ reference system is attached and to the mobile platform - the $oxyz$ own reference system (figure 1). The mobile plate pose in space is given by the position vector $\overline{Oo}$ of the "o" platform centre, $\overline{P} = \overline{P}(X,Y,Z)$ and through the rotational matrix: $[R] = [R(\alpha,\beta,\gamma)]$.

In the case of "a" type mechanisms the absolute coordinates of the $A_i (i = 1,2,3)$ points depend on the actuated coordinates q_i from B_i joints and passive coordinates u_i from C_i joints:

$$X_i = X_i(q_i,u_i); Y_i = Y_i(q_i,u_i); Z_i = Z_i(q_i,u_i); \quad i = 1,2,3 \tag{1}$$

By eliminating the passive joint coordinates u_i, the Cartesian equations of the described curves by the A_i points in the fixed frame are obtained:

$$F_i(X_i,Y_i,Z_i) = 0 \tag{2}$$

$$G_i(X_i,Y_i,Z_i,q_i) = 0 \tag{3}$$

For the "b" type mechanisms the $A_i (i = 1,2,3)$ absolute coordinates depend only on the actuated joint coordinates q_i while the relative coordinates of the $A_i (i = 1,2,3)$ points, in *oxyz* reference system, depend on the passive joint coordinates u_i:

$$X_i = X_i(q_i);\ Y_i = Y_i(q_i);\ Z_i = Z_i(q_i) \tag{4}$$

$$x_i = x_i(u_i);\ y_i = y_i(u_i);\ z_i = z_i(u_i) \tag{5}$$

By eliminating joints coordinates q_i from (4) and u_i from (5), the Cartesian equations of the described curves by the A_i points in the fixed frame and in the mobile frame are obtained:

$$F_i(X_i,Y_i,Z_i) = 0;\ \ G_i(X_i,Y_i,Z_i) = 0;\ i = 1,2,3 \tag{6}$$

$$f_i(x_i,z_i,y_i) = 0;\ \ g_i(x_i,z_i,y_i) = 0;\ i = 1,2,3 \tag{7}$$

The direct geometric model (DGM) assumes to impose the drive joint coordinates $q_i (i = 1,2,3)$ and to obtain the mobile platform pose through the X, Y, Z coordinates of the mobile plate centre and the α, β, γ orientation angles.

The closure equations for the DGM are represented by the equality of the distances between the guiding points in these two reference systems:

$$\left|\overline{P}_j - \overline{P}_i\right| = \left|\overline{p}_j - \overline{p}_i\right|; \quad (i, j) = (1,2), (2,3), (3,1) \qquad (8)$$

Through numerical solution of the nonlinear equation system (8) the passive joint coordinates u_i are obtained.

In the case of "a" type mechanisms the absolute coordinates of the guiding points with (1) and then the position of the "o" point and the mobile platform orientation are computed.
In the case of "b" type mechanisms the relative coordinates of the same points are computed with (5) and then from the system:

$$\left(\overline{P}_i - \overline{P}\right)^2 = \overline{p}_i^{\,2}; \; i = 1,2,3 \qquad (9)$$

which allows explicit solution, are computed the X, Y, Z coordinates of the mobile platform center and subsequently the mobile platform orientation.

The inverse geometrical model (IGM) assumes to impose the mobile platform coordinates and to compute the drive joint coordinates.

As the mechanism has only 3 DOF, the main problem is to define three implicit functions, which connect the variables $X, Y, Z, \alpha, \beta, \gamma$. Establishment of theses implicit functions is different for the mechanisms "a" and "b".

In the case of mechanism of type "a", the implicit function system is given by the equations (2) of the fixed surfaces, on which the points A_i are moving. In these equations the variables X_i, Y_i, Z_i are replaced by their expressions with respect to the Cartesian coordinates of the mobile plate:

$$\begin{bmatrix} X_i & Y_i & Z_i \end{bmatrix}^T = \begin{bmatrix} X & Y & Z \end{bmatrix}^T + [R]\begin{bmatrix} x_i & y_i & z_i \end{bmatrix}^T \qquad (10)$$

It yields:

$$H_i = H_i(X, Y, Z, \alpha, \beta, \gamma) = 0 \qquad (11)$$

In the case of mechanism of type "b" the determination of the implicit functions is much more complicated.

Relative coordinate expressions with respect to the absolute ones are replaced in (7):

$$\begin{bmatrix} x_i & y_i & z_i \end{bmatrix}^T = [R]^T \begin{bmatrix} X_i - X & Y_i - Y & Z_i - Z \end{bmatrix}^T \qquad (12)$$

and it yields the equations of the curves Γ_i' in the fixed base reference system, which are jointed to the mobile plate:

$$f_i(X_i, Y_i, Z_i, X, Y, Z, \alpha, \beta, \gamma) = 0; \; i = 1,2,3 \qquad (13)$$

$$g_i(X_i, Y_i, Z_i, X, Y, Z, \alpha, \beta, \gamma) = 0; \; i = 1,2,3 \qquad (14)$$

The implicit functions are obtained through association of the equations (6), (13) and

(14) and elimination of the X_i, Y_i, Z_i variables:

$$H_i \equiv H_i(X, Y, Z, \alpha, \beta, \gamma) = 0; \quad i = 1, 2, 3 \tag{15}$$

The determination of the main and secondary coordinates triplet is performed through the calculus of the $C_6^3 = 20$ Jacobians of the functions H_1, H_2, H_3 with respect to three variables from the six Cartesian coordinates *X, Y, Z,* α, β, γ of the mobile plate.

In the "a" case, if the guiding points are imposed to remain in arbitrary planes, then the implicit functions are linear functions with respect to the X, Y, Z variables:

$$H_i \equiv a_i X + b_i Y + c_i Z + d_i + e_i(\alpha, \beta, \gamma) = 0; i = 1,2,3 \tag{16}$$

The Jacobian, which corresponds to the X, Y, Z triplet is in this case constant:

$$\frac{D(H_1, H_2, H_3)}{D(X, Y, Z)} = \begin{vmatrix} a_1 & b_1 & c_1 \\ a_2 & b_2 & c_2 \\ a_3 & b_3 & c_3 \end{vmatrix} \tag{17}$$

If the Jacobian is also non-zero, then the secondary position coordinates could be expressed with respect to the main orientation coordinates:

$$X = X(\alpha, \beta, \gamma); Y = Y(\alpha, \beta, \gamma); Z = Z(\alpha, \beta, \gamma) \tag{18}$$

A particular case of the "a" type mechanisms is presented in figure 2 when the guiding points form an equilateral triangle and they must remain in the planes which contain the OZ axis, symmetrical disposed at 120^0 (the first plane is XOZ), then the main coordinates are Z, α, β and the secondary are X, Z, γ . If $[R] = [R_{x(\alpha),y(\beta),x(\gamma)}]$ then:

$$X = \frac{1}{2} r\left[\left(1 + s^2\alpha\right)c\beta - c^2\alpha\right]; Y = -r\, s\alpha\, s\beta; \; \gamma = \alpha, \tag{19}$$

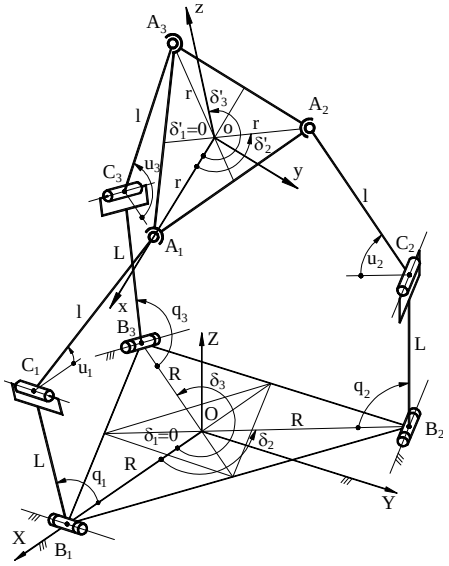

Fig. 2. The 3-RRS parallel mechanism

Generally, the computing of the secondary coordinates of the mobile platform is made through the solution of the implicit equation system.

In the case "a" the actuating joint coordinates q_i result from the equations (3) and in the case "b" the actuating joint coordinates q_i result from (4).

The kinematic model is obtained for the same 3-RRS mechanism (figure 2) through the differentiation of the vector form of the input-output equations:

$$\left(\overline{P}_i - \overline{P}_{C_i}\right)^2 - l^2 = 0;\ i = 1,2,3 \tag{20}$$

The kinematic model will be:

$$[A]\dot{\overline{X}} = [B]\dot{\overline{q}}\ , \tag{21}$$

where, $\dot{X} = [\dot{\varphi}, \dot{\theta}, \dot{Z}]$; $\dot{\overline{q}} = [\dot{q}_1, \dot{q}_2, \dot{q}_3]$

$$[A] = \begin{bmatrix} (\overline{P}_1 - \overline{P}_{C_1}) \cdot \dfrac{\partial \overline{P}_1}{\partial \alpha} & (\overline{P}_1 - \overline{P}_{C_1}) \cdot \dfrac{\partial \overline{P}_1}{\partial \beta} & (\overline{P}_1 - \overline{P}_{C_1}) \cdot \dfrac{\partial \overline{P}_1}{\partial Z} \\ (\overline{P}_2 - \overline{P}_{C_2}) \cdot \dfrac{\partial \overline{P}_2}{\partial \alpha} & (\overline{P}_2 - \overline{P}_{C_2}) \cdot \dfrac{\partial \overline{P}_2}{\partial \beta} & (\overline{P}_2 - \overline{P}_{C_2}) \cdot \dfrac{\partial \overline{P}_2}{\partial Z} \\ (\overline{P}_3 - \overline{P}_{C_3}) \cdot \dfrac{\partial \overline{P}_3}{\partial \alpha} & (\overline{P}_3 - \overline{P}_{C_3}) \cdot \dfrac{\partial \overline{P}_3}{\partial \beta} & (\overline{P}_3 - \overline{P}_{C3}) \cdot \dfrac{\partial \overline{P}_3}{\partial Z} \end{bmatrix};$$

$$[B] = L \cdot l \begin{bmatrix} s(u_1 - q_1) & 0 & 0 \\ 0 & s(u_2 - q_2) & 0 \\ 0 & 0 & s(u_3 - q_3) \end{bmatrix};$$

$$\overline{P}_{C_i} = \overline{OC_i}$$

Workspace Analysis

For workspace mechanisms generation three methods are well-known:
1. Method which uses the inverse geometrical model;
2. Method which uses the direct geometrical model;
3. Method in which the Cartesian workspace results as an intersection of the workspace for each kinematical chain.

In this paper the workspace analysis is performed in "mixed" coordinates, because this mechanism will be used for orientation applications.

Thus, we intend to find out the workspace in operational coordinates α, β, Z , so-called "pseudo-space", because it can be for it a volume in geometrical sense.

The MGI Method

Using this method, we can determine the points that belong to the working pseudo-sections from the "$\alpha\beta$" planes at successive levels of "Z". The algorithm of this method is as follow:

- the level of the center of the mobile platform is imposed:
$Z(p) = Z_{min} + p \cdot pasZ$, where $p = 0,...n_p$;
- the plane "$\alpha\beta$" at the Z(p) level is scanned:
$\alpha(j) = \alpha_{min} + j \cdot pas\alpha$, where $j = 0,..., n_j$;
$\beta(k) = \beta_{min} + k \cdot pas\beta$, where $k = 0,..., n_k$;
- the absolute coordinates of the spherical joints coordinates are calculated;
- the closure equations coefficients "$a_i cq_i + b_i sq_i = c_i$"
are calculated;
- the first constraint is verified: $\Delta_i \equiv a_i^2 + b_i^2 - c_i^2 \geq 0$
- the actuating joint coordinates are calculated:

$$q_i = atan2\frac{sq_i}{cq_i}; \quad i = 1,2,3$$

- the second constraint is calculated:
$q_{min} \leq q_i \leq q_{max}$; $i=1,2,3;$
- the passive joint coordinates u_i could be computed;
- the rotation angle from the spherical joint is computed:

$$c\theta_i = \begin{bmatrix} c\delta_i\, cu_i \\ s\delta_i\, cu_i \\ -su_i \end{bmatrix} \cdot [R] \cdot \begin{bmatrix} c\delta_i\, cu_0 \\ s\delta_i\, cu_0 \\ -su_0 \end{bmatrix}; \; i = 1,2,3; \; u_0 = a\cos\frac{R-r}{l}$$

- the third constraint is verified (only for real joints):

$$c\theta_i \geq \cos(\theta_0); \theta_0 = \frac{\pi}{4}$$

If all the constraints are verified, the triplet (j,k,p) is valid, which has the coordinates α_j, β_k, Z_p. The point $P_{jkp} = P(\alpha_j, \beta_k, Z_p)$ is represented in the pseudo-space of the coordinates "$\alpha\ \beta\ Z$". The robot pseudo-space consists of all valid points.

The MGD method

Using this method we calculate the conventional points defined by the coordinates α, β, Z, which can be reached by the mobile platform. The point cloud represents the robot pseudo-workspace.

The algorithm of this method is as follow:
- the actuating joint coordinates space is scanned:

$$q_1(j) = q_{min} + j \cdot pasq; \quad q_2(k) = q_{min} + k \cdot pasq;$$
$$q_3(p) = q_{min} + p \cdot pasq; \quad j,k,p = 0,...,n;$$

- for every triplet (j,k,p) the system of the input-output equations is solved;
- thus, n^3 conventional points $P_{jkp} = P(\alpha_j, \beta_k, Z_p)$ are obtained, which are represented in the coordinate system $\alpha\ \beta\ Z$.

Singularity Analysis

According to [13] there are three singularity types. **First type of singularities** occurs when the det(B**)** = 0, which means the case when active and passive joint coordinates are equal: $q_i = u_i$; i =1,2,3. This configuration has a practical interpretation: the arms and the guiding bars for the kinematical chains are collinear. **Second type of singularities** occurs when the det(A**)** = 0. Geometrically, these singularities are encountered in the configurations where the guiding bars are in the mobile platform plane. The **third type of singularities**, so-called architectural singularities, is present when both Jacobian determinants are zero. These types of singularities can be easily avoided in the design stage.

Dynamic Analysis

The dynamics consists of finding the relationships between the actuating joint torques Q_i (i=1,2,3) and the laws of motion of the mobile plate.

The same 3-RRS parallel mechanism used for orientation is considered, that is with the base lied on the vertical wall, the X axis oriented to the top and the Z axis oriented to the south. If $[R] = [R_{x(\alpha),y(\beta),z(\gamma)}]$ then the $\alpha = \varphi$ and $\beta = \theta$ are the azimuth and elevation angles.

In the dynamic study, several simplifying hypotheses were adopted: firstly, all joints frictionless and secondly, the inertia of guiding arms A_iC_i is neglected.

The mechanism dynamics using the Newton-Euler laws is performed into two steps: In the first step the upper part of the structure containing the working platform and dish is separated from the rest of the mechanism (figure 3).

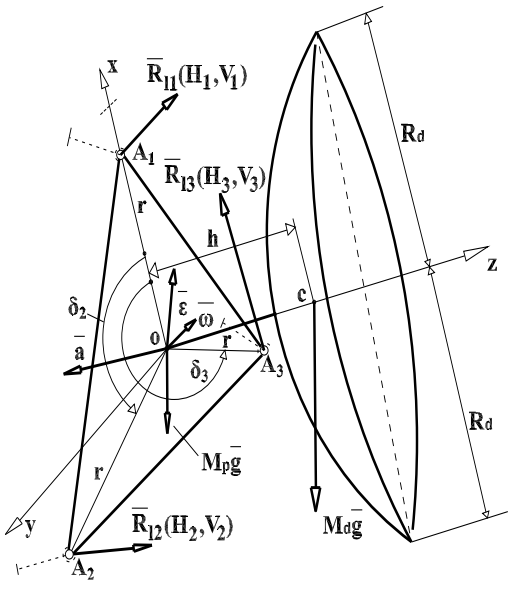

Fig. 3. Step 1

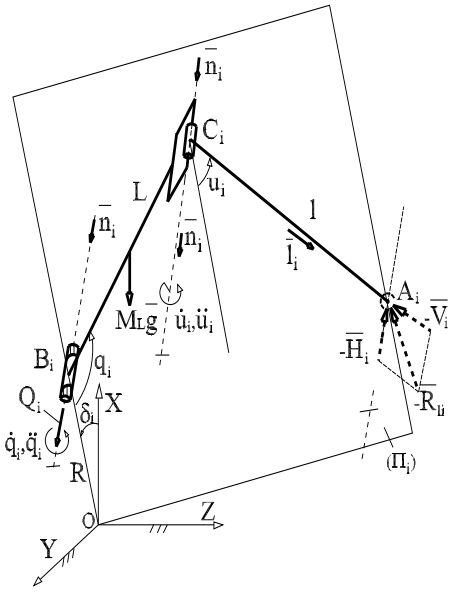

Fig. 4. Step 2

The Newton-Euler equations, which are modeling the motion of the mobile working platform and dish, allow the determination of the spherical joints reaction components $\overline{H}(H_1,H_2,H_3)$ and $\overline{V}(V_1,V_2,V_3)$. In the second step, the $B_iC_iA_i$ kinematic chain is separated and all forces are introduced (figure 4). The moment equation relative to the B_i joint axis allows finding the active torque Q_i:

$$Q_i = -V_i L\, s(q_i - u_i) + \frac{M_L L^2}{3}\ddot{q}_i + M_L g \frac{L}{2} s q_i\, c\delta_i; i = 1,2,3 \qquad (22)$$

where M_L is mass of B_iC_i link.

For the friction forces approximation the model of the viscous friction together with the model of Coulomb friction is chosen. A friction torque in a passive joint is a vector situated along the relative rotational speed of the considered link with respect to the previous link (belonging to the same kinematic chain) (figure 5):

$$\overline{M}_{fC_i} = -(c_r + \mu_r \frac{d_r}{2}\frac{|V_i|}{|\dot{u}_i - \dot{q}_i|})(\dot{\bar{u}}_i - \dot{\bar{q}}_i) = -k_{ri}(\dot{\bar{u}}_i - \dot{\bar{q}}_i) \qquad (23)$$

$$\overline{M}_{fA_i} = -(c_s + \mu_s \frac{d_s}{2}\frac{\sqrt{H_i^2 + V_i^2}}{|\overline{\omega} - \dot{u}_i \bar{n}_i|})(\overline{\omega} - \dot{\bar{u}}_i) = -k_{S_i}(\overline{\omega} - \dot{\bar{u}}_i) \qquad (24)$$

In the B_i active point the friction torque is:

$$\overline{M}_{fB_i} = -(c_R + \mu_R \frac{d_R}{2}\frac{\sqrt{V_i^2 + (M_L g c\delta_i)^2 + 2V_i M_L g c\delta_i c u_i}}{|\dot{q}_i|})\dot{\bar{q}}_i = -k_{R_i}\dot{\bar{q}}_i \qquad (25)$$

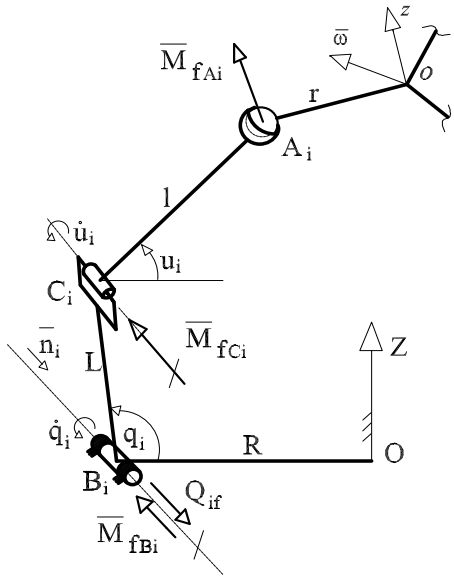

Fig. 5. The friction torques

H_i, V_i - reaction force component from the spherical joint A_i; c_s, c_r, c_R - viscous coefficient from spherical joint, passive joint and active joint; μ_s, μ_r, μ_R - Coulomb friction coefficients from the same joints; d_r, d_R - diameters of the rotational joint spindle; d_s - diameter of the spherical joint ball; $\overline{n}_i$ - unit vector of B_i and C_i axes; $\overline{\omega}$ - absolute angular speed of the mobile plate; $\dot{\overline{q}}_i = \dot{q}_i \overline{n}_i$ and $\dot{\overline{u}}_i = \dot{u}_i \overline{n}_i$ - absolute angular speed of B_iC_i and respectively C_iA_i link.

In order to get the drive torques which are necessary to overcome the frictions from the joints **the principle of virtual power** is applied.

$$\overline{Q_f} \cdot \dot{\overline{q}} + \sum_{i=1}^{3} \overline{M}_{fB_i} \cdot \dot{\overline{q}}_i + \sum_{i=1}^{3} \overline{M}_{fC_i} \cdot (\dot{\overline{u}}_i - \dot{\overline{q}}_i) + \sum_{i=1}^{3} \overline{M}_{fA_i} \cdot (\overline{\omega} - \dot{\overline{u}}_i) = 0 \qquad (25)$$

Finally it yields:

$$\begin{bmatrix} Q_{1f} \\ Q_{2f} \\ Q_{3f} \end{bmatrix} = \begin{bmatrix} k_{R1}\dot{q}_1 + k_{r1}(\dot{q}_1 - \dot{u}_1) \\ k_{R2}\dot{q}_2 + k_{r2}(\dot{q}_2 - \dot{u}_2) \\ k_{R3}\dot{q}_3 + k_{r3}(\dot{q}_3 - \dot{u}_3) \end{bmatrix} + [J_u]^T \begin{bmatrix} k_{r1}(\dot{u}_1 - \dot{q}_1) + k_{s1}(\dot{u}_1 - 2\overline{\omega} \cdot \overline{n}_1) \\ k_{r2}(\dot{u}_2 - \dot{q}_2) + k_{s2}(\dot{u}_2 - 2\overline{\omega} \cdot \overline{n}_2) \\ k_{r3}(\dot{u}_3 - \dot{q}_3) + k_{s3}(\dot{u}_3 - 2\overline{\omega} \cdot \overline{n}_3) \end{bmatrix} + (k_{s1} + k_{s2} + k_{s3})[J_\omega]^T \begin{bmatrix} \omega_X \\ \omega_Y \\ \omega_Z \end{bmatrix} \qquad (26)$$

where $[J_u]$ and $[J_\omega]$ are Jacobi matrices that connect the passive joints velocities vector $\dot{\overline{u}}$ and the angular velocity $\overline{\omega}$ of the mobile platform to the velocity vector of active joints.
The total generalized forces will be:

$$Q_{im} = Q_i + Q_{if} \qquad (27)$$

Simulation Tests

As an application, a parallel mechanism 3-RRS with the following design data is considered:

$R = 0.45\,m;\ L = 0{,}40m;\ l = 0{,}60m;\ r = 0.15m$
$\delta_1 = \delta_1' = 0°;\ \delta_2 = \delta_2' = 120°;\ \delta_3 = \delta_3' = 240°$

For the workspace representation, a program using IGM has been developed. By means of this program the pseudo-sections "αβ" at different levels of $Z \in [Z_{min}, Z_{max}]$ can be represented;

$$Z_{min} = \sqrt{(L)^2 - (l + r - R)^2}\ ,\ Z_{max} = \sqrt{(L + l)^2 - (R - r)^2}$$

The program has a graphical interface, which allows the choice between the section visualization within the workspace, using real or ideal joints.

Figure 6 demonstrates section visualization at Z=74.71 cm and Z=81.61 cm using real joints. The maximal areas are obtained for values of Z in the range of 74-82 cm.

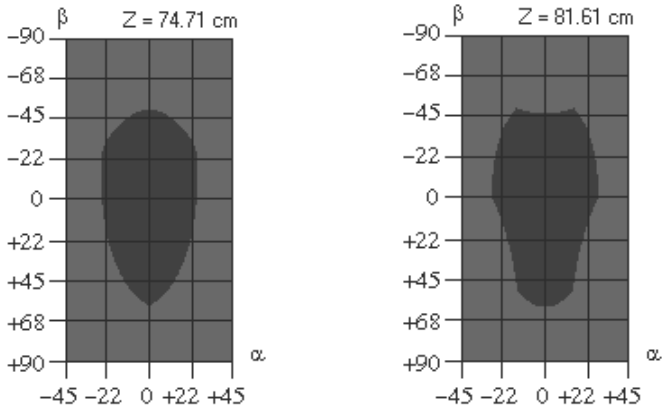

Fig. 6. Section visualization using real joints

For the singularity identification, the graphical representation of the surface given by an implicit equation det(A**)** = 0 is difficult, the Z-coordinate is imposed and the level curves (isohypses) of the determinants are represented. In the figure 7 the level curves respectively the singularities curves (with the ”0” values) are illustrated. These curves represent the values of the Jacobi matrix determinant A for different values of Z coordinate.

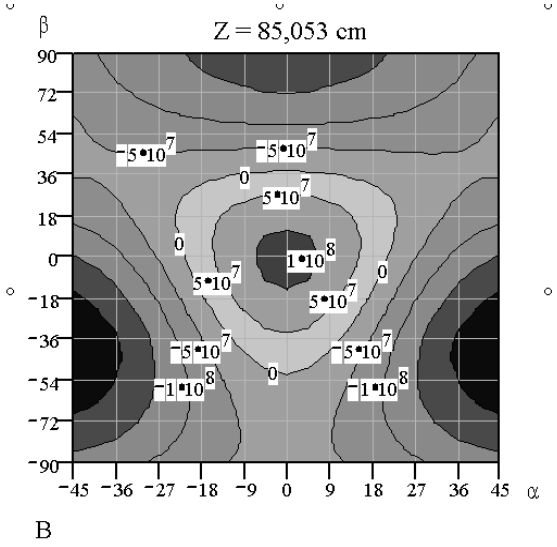

Fig. 7. The level curves of det(A)

Regarding the dynamics, the chosen inertia data for the parallel mechanism are: $\rho = 0.136m;\ M = 8.8kg,\ M_L = 0.5kg;\ I_x = I_y = 0.57kg \cdot m^2;\ I_z = 0.5\,kg \cdot m^2$. The selected displacement of the working platform has the equations:

$$\begin{cases} Z = 0.85\,m \\ \varphi_k = \dfrac{\pi}{6} \sin \lambda_k,\ \ \theta_k = \dfrac{\pi}{6} \cos \lambda_k,\ \ k = 1,2,...,8 \end{cases}$$

$$\begin{cases} \lambda_k = -\dfrac{2^{11}}{27\pi^2}\left(\dfrac{t_k}{k}\right)^3 + \dfrac{2^7}{3\pi}\left(\dfrac{t_k}{k}\right)^2; \quad t_k = \left[0, k\dfrac{3\pi}{8}\right] s \\ \tau_k = \dfrac{t_k}{t_{k\,max}} = \dfrac{t_k}{k\dfrac{3\pi}{8}}; \quad \tau_k \in [0,1] \ \ normalized\ \ time \end{cases}$$

Considering friction effect the input data are:

$$d_r = 0.01;\ d_R = 0.012;\ d_s = 0.016; \quad c_r = c_s = 0.02;\ c_R = 0.04;$$

$$\mu_{r,R} = (\mu + \frac{2s}{d_{r,R}})/(\sqrt{1+\mu^2}); \qquad \mu = 0.2\ ;\ s = 0.0005$$

The center of mobile plate for all k = 1,2,…,8 laws describes in the plane $Z = 0.85m$ a pseudo-ellipse with the semi axes $9.97 \cdot 10^{-3} m$ and $9.78 \cdot 10^{-3} m$. The generalized torques Q_{im} have been evaluated for all k motion laws.

In the figures 8 and 9 are presented the generalized force diagrams for k = 2 si 4.

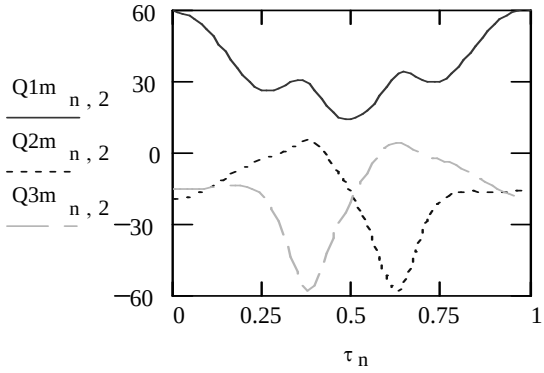

Fig. 8. Generalized torques for k=2

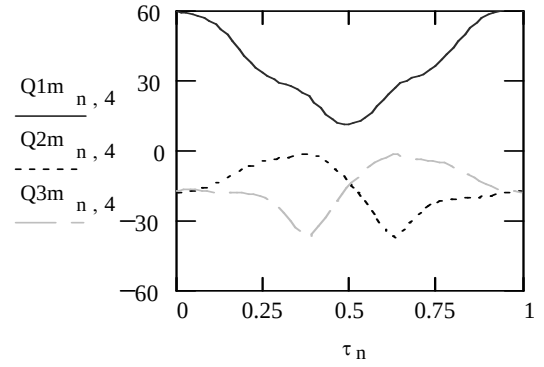

Fig. 9. Generalized torques for k=4

Conclusions

Unitary approach encompassing some classes of 3-DOF parallel robots with triangular platform was proposed in this paper. Geometrical models for two parallel mechanisms types guided in three points and having three degrees of freedom were compared in the reported study. The obtained results indicate that in the case of "a" type mechanisms the expressions for the geometrical model and the implicit equations form are less complex in comparison to the case of "b" type mechanisms. This leads to the conclusion that it is recommended to build parallel robots of type "a".

The solution obtained for the system proposed herein to determine the workspace and singularities for this parallel structure can be generalized to some other parallel structures or parallel robots with three degrees of freedom. Possible applications of the studied 3-RRS parallel structure are antenna orientation or sun tracker.

Kinematic and dynamic modeling of a 3-DOF parallel mechanism for orientation applications are also presented in the paper. Dynamic models with and without friction were obtained. Diagrams for the dynamics representation were determined using numerical as well as graphical simulations.

Acknowledgments

The authors gratefully acknowledge the financial support provided by the research grants awarded by the Romanian Ministry of Education and Research.

References

[1] Plitea N. Umgekherte Lageaufgabe von Raeumlichen Parallelgetrieben der Industrieroboter mit Drei Freiheitsgraden vom Typ a, in Proc. 3rd National Conference of Precision Engineering and Optics, COMEFIN 3, Brasov, Romania, vol. I: 221-228, (1991).

[2] Lee K.-M., Shah D. K. Kinematic Analysis of a Three-Degrees-of-Freedom In-Parallel Actuated Manipulator, IEEE Journal of Robotics and Automation, (4), 3: 354-360, (1988).

[3] Bulca F., Angeles J. and Zsombor-Murray P. J. On the Workspace determination of spherical serial and platform mechanisms, Mech. and Mach. Theory, vol. 34: 497-512, (1999).

[4] M. Ceccarelli, A Formulation for the Workspace boundary of General N-Revolute Manipulators, Mech. and Machine Theory, (31), 5: 637-646,(1996).

[5] Chablat D. and Wenger Ph. Workspace Analysis of the Orthoglide using Interval Analysis, in Advances in Robot Kinematics, J.lenarcic and F. Thomas Eds., Kluver Academic, pp. 397-406, (2002).

[6] Gosselin C. Determination of the Workspace of 6-dof parallel manipulators. ASME Journal of Mechanical Design, vol. 112-3, pp. 331-336, (1990).

[7] Husty M. L. On the workspace of planar three-legged platforms, in World Automation Congress, vol. 3, Montpelier pp. 339-344, (1996).

[8] Pernkopf F., Husty M. Reachable Workspace and Manufacturing Errors of Stewart-Gough Manipulators, Proc. of. MUSME 2005, Brazil, (2005).

[9] Itul T., Pisla D. L. Workspace Analysis of a Three Degrees of Freedom Parallel Robot, in IEEE 2006 IEEE-TTTC International Conference on Automationa, Qualitz and Testing, Robotics, AQTR 2006, tome II, pages 290-295, Cluj-Napoca, (2006).

[10] Merlet, J.-P. Parallel robots, Kluwer Academic Publisher, (2000).

[11] Pernkopf F., Husty M. L. Singularity-Analysis of Spatial Stewart-Gough Platforms with planar base and platform, in DETC2002/MECH-34267, ASME Design Engineering Technical Conferences, Montreal, Canada, (2002).

[12] Sefrioui J. and Gosselin C. M. Étude et reprézentation des lieux de singularité des manipulateurs parallèles spheriques à trois degrés de liberté avec actionneurs prismatiques, Mechanism and Machine Theory, 29(4): 559–579, (1994).

[13] Gosselin C. M. and Wang J. Singularity loci of planar manipulators with revolute actuators, Robotics and Autonomous Systems Elsevier Science, Vol. 21: 377-398, (1997).

[14] Grotjahn M., Heimann B. and Abdellatif H. Identification of friction and Rigid-Body Dynamics of Parallel Kinematic Structures for Model-Based Control, in Multibody System. Dynamics, (11)3: 273-294, (2004).

[15] Poignet Ph., Ramdani N. and Vivas O. A. Robust estimation of parallel robot dynamic parameters with interval analysis, In. 42nd IEEE Conference on Decision and Control, pp. 6503-6508, Hawaii USA, (2003).

[16] Chen J.-S., Yao-Hung Kuo, Hsu W-Y. The influence of friction on contouring accuracy of a Cartesian guide tripod machine tool, Int. J. Adv. Manuf. Technol., 30: 470-478, (2006).

[17] T. Itul, D. Pisla and A. Pisla, Dynamic Model of a 6-DOF Parallel Robot by Considering Friction Effects, in 12th IFToMM World Congress, Besançon (France), June 18-21, CD-ROM edition, (2007).

[18] Guégan S. and Khalil W. Dynamic modeling of the orthoglide. Advances in robot kinematics (J.Lenarcic and F. Thomas, Ed.), Kluver Academic, Publication, Netherlands, pp. 387-396, (2002).

[19] Poignet Ph., Ramdani N., Vivas O. A. Robust estimation of parallel robot dynamic parameters with interval analysis, In. 42nd IEEE Conference on Decision and Control, Hawaii USA, pp. 6503-6508, (2003).

[20] Itul T., Pisla D. The Influence of Friction on the Dynamic Model for a 6-DOF Parallel Robot with Triangular Platform, Journal of Vibroengineering 2007, October/December, (9), 4: 24-29, (2007).